European Journal of Phycology

ISSN: 0967-0262 (Print) 1469-4433 (Online) Journal homepage: www.tandfonline.com/journals/tejp20

Multi-generation dispersal shapes the genetic structure of the canopy-forming seaweed *Ericaria amentacea* (syn. *Cystoseira amentacea*) in the north-western Mediterranean Sea

Lauric Reynes, Térence Legrand, Aurélie Blanfuné, Jorge Assis, Thierry Thibaut & Lorraine Bottin

To cite this article: Lauric Reynes, Térence Legrand, Aurélie Blanfuné, Jorge Assis, Thierry Thibaut & Lorraine Bottin (23 Sep 2025): Multi-generation dispersal shapes the genetic structure of the canopy-forming seaweed *Ericaria amentacea* (syn. *Cystoseira amentacea*) in the north-western Mediterranean Sea, European Journal of Phycology, DOI: 10.1080/09670262.2025.2554068

To link to this article: https://doi.org/10.1080/09670262.2025.2554068

EUROPEAN JOURNAL OF PHYCOLOGY, 2025
https://doi.org/10.1080/09670262.2025.2554068

British Phycological Society
Understanding and using algae

Taylor & Francis
Taylor & Francis Group

Multi-generation dispersal shapes the genetic structure of the canopy-forming seaweed *Ericaria amentacea* (syn. *Cystoseira amentacea*) in the north-western Mediterranean Sea

Lauric Reynes[a,b], Térence Legrand[c], Aurélie Blanfuné[a], Jorge Assis[c,d], Thierry Thibaut[a] and Lorraine Bottin[e]

[a]CNRS, IRD, Mediterranean Institute of Oceanography, Aix Marseille Université, Université de Toulon, Marseille 13288, France; [b]School of Life Sciences, University of Hawaii at Mānoa, Honolulu, Hawaii 96822, USA; [c]Centre of Marine Sciences (CCMAR-Algarve), University of Algarve, Faro 8005-139, Portugal; [d]Faculty of Bioscience and Aquaculture, Nord Universitet, Bodø 8049, Norway; [e]ECOSEAS, CNRS, Faculté des Sciences, Université Côte d'Azur, Nice cedex 2, Parc Valrose 06108, France

ABSTRACT
Canopy-forming seaweeds, especially fucoids (Fucales, Phaeophyceae), constitute marine forests in the Mediterranean Sea that deliver key ecosystem services. However, escalating human pressures in coastal areas have led to habitat fragmentation, significantly impacting the dynamics of gene flow and evolutionary trajectories. In this study, we investigated population connectivity among 43 sites with *Ericaria amentacea* in the northwestern Mediterranean Sea. By integrating microsatellite genotyping and biophysical modelling, we aimed to evaluate the hypothesis that population connectivity is approximated by oceanographic connectivity, rather than coastal distance. While traditional approaches to oceanographic connectivity had focused on single-generation dispersal models, we adopted a multi-generation perspective. This involves employing a biophysical model that considers gene flow through multiple stepping-stone populations across the *E. amentacea* distribution and over distinct generations of dispersal. Using distance-based redundancy analysis (dbRDA), we found that multi-generation dispersal significantly contributes to genetic differentiation, surpassing the influence of coastal distance. Even so, genetic differentiation remained significant among all population pairs, suggesting that gene flow may be hindered by differential selection acting against migrants and/or obscured by the effects of local genetic drift. The latter is likely, given the species' low dispersal potential and self-compatibility, both of which promote small, spatially restricted breeding units. In addition, our results emphasized that oceanographic connectivity promoted long-distance dispersal across northern Corsica and Eastern Provence over a single generation through the drifting of fertile thalli, which might have contributed to moderate differentiation between local populations. Overall, this framework highlights the value of considering multi-generation dispersal across numerous intermediate stepping-stones for informing management strategies aimed at enhancing population connectivity and safeguarding genetic diversity in seaweeds.

HIGHLIGHTS
- Genetic differentiation in *Ericaria amentacea* persists despite frequent dispersal events.
- Oceanographic connectivity shapes genetic structure.
- Multi-generation dispersal is pivotal for understanding connectivity in macroalgae.

ARTICLE HISTORY Received 10 July 2024; Revised 20 August 2025; Accepted 21 August 2025

KEYWORDS Fucoids genetic structure; long-distance dispersal; microsatellites; population connectivity; stepping-stones

Introduction

Marine forests are the primary rocky coastal ecosystems in the pristine environments of temperate and cold oceans (Steneck *et al.*, 2002). In particular, kelps and fucoids are vital components of these ecosystems, supporting diverse functional compartments and trophic levels. These canopy-forming seaweeds provide habitat, food and nursery grounds for various marine organisms, including invertebrates, fish and marine mammals. However, kelps and fucoids are experiencing dramatic declines globally, a phenomenon driven directly or indirectly by human activities (e.g. Hanley *et al.*, 2024; Manca *et al.*, 2024). In the Mediterranean Sea, canopy-forming seaweeds are represented mainly by the genus *Cystoseira* sensu lato (Fucales, Phaeophyceae), species of which dominate rocky reef assemblages from the littoral fringe down to the lower sublittoral zone. The decline of these species has been reported all around the Mediterranean Sea, varying between populations and regions. Their decline is a consequence of habitat destruction, eutrophication and overgrazing by herbivores, leading to a shift to reduced structural complexity (e.g. Devescovi & Ivesa, 2007; Fraschetti *et al.*, 2011; Thibaut *et al.*, 2014; Blanfuné *et al.*, 2016*a*, *b*; Gianni *et al.*, 2017). These shifts are associated with a collapse of biodiversity and ecosystem function and services (Sala & Knowlton, 2006; Thibaut *et al.*, 2015; Eger *et al.*, 2023).

CONTACT Lauric Reynes ✉ lreynes@hawaii.edu

Ericaria amentacea (C.Agardh) Molinari & Guiry belongs to a species complex which includes *E. selaginoides* (Linnaeus) Molinari & Guiry (formerly *Cystoseira tamariscifolia* (Hudson) Papenfuss) and *E. mediterranea* (Sauvageau) Molinari & Guiry (Feldmann, 1937). This complex is characterized by considerable morphological variability and low genetic differentiation (Bermejo *et al.*, 2018). Bruno de Sousa *et al.* (2019) placed *E. amentacea* within the *Cystoseira-I* clade, alongside *E. tamariscifolia* and *E. mediterranea*. While *E. mediterranea* is resolved as a distinct entity, the other two species are poorly differentiated genetically (Neiva *et al.*, 2022). These species can be observed in sympatry in some regions, such as the Alboran Sea (Blanfuné *et al.*, 2019, 2022), but *E. amentacea* is restricted to the French Riviera, Provence and Corsican coastlines (Thibaut *et al.*, 2014; Blanfuné *et al.*, 2022), with no recorded observations of the *E. mediterranea* or *E. selaginoides* morphotypes in over 200 years of phycological research in these regions. Beyond the ongoing debate over the discordance between genetic entities and morphotypes, *E. amentacea* deserves particular attention, as its populations are experiencing a marked decline in the northern Mediterranean Sea, despite its high ecological status within the framework of the EU Water Framework Directive (2000/60/EC) (e.g. Blanfuné *et al.*, 2016*a*, 2017). This decline has been attributed to significant eutrophication and habitat destruction, which accelerate fragmentation and population isolation (Thibaut *et al.*, 2014; Blanfuné *et al.*, 2022).

Population genetic connectivity, describing the extent and directionality of gene flow among populations, is instrumental for informing conservation and management efforts in spatially subdivided marine forests (e.g. Coleman & Kelaher, 2009; Couceiro *et al.*, 2013; Capdevila *et al.*, 2018; Durrant *et al.*, 2018; Fouqueau *et al.*, 2024; Minne *et al.*, 2025). Gene flow is one of the main evolutionary forces shaping genetic variation within and between populations (Slatkin, 1985, 1987), with outcomes that can be beneficial or, in some cases, deleterious for population persistence. Deleterious effects may occur when gene flow homogenizes the gene pool, leading to the loss of variants that could confer higher fitness and survival in distinct environments (Ronce & Kirkpatrick, 2001; Lenormand, 2002). Low to moderate gene flow can still be beneficial by limiting inbreeding and facilitating the spread of advantageous variants among populations facing similar selective pressures. Gene flow between spatially subdivided populations of *Cystoseira* sensu lato species has traditionally been considered limited, given the short dispersal distances of zygotes, typically spanning only a few dozen centimetres (Mangialajo *et al.*, 2012) to up to 10 metres (Capdevila *et al.*, 2018). However, long-distance dispersal events have been revealed by observations of *Cystoseira* s.l. populations newly establishing on man-made structures located far from other known populations (Thibaut *et al.*, 2014), indicating that long-distance gene flow may be achieved. The most plausible explanation is dispersal mediated by sea-surface rafting of fertile thallus fragments, which is further supported by seascape genetics studies, showing that genetic differentiation is better explained by dispersal mediated by ocean currents than geographic distance, such as in *E. amentacea* (Thibaut *et al.*, 2016; Buonomo *et al.*, 2017) and *E. zosteroides* (Reynes *et al.*, 2021*a*). However, dispersal has traditionally been considered through single-generation connectivity events (e.g. Durrant *et al.*, 2018; Fouqueau *et al.*, 2024), whereas biophysical models incorporating a multi-generation perspective have more recently offered improved support for explaining genetic structure in sessile organisms, including macroalgae (Legrand *et al.*, 2022, 2024). This approach accounts for several generations of migrants, with each intermediate, connected population functioning as a stepping-stone. Its benefit lies in the fact that, for macroalgae, it better models dispersal among spatially subdivided populations, even those not genetically sampled, and it considers long-distance dispersal through the rafting of fertile thallus, thereby offering deeper insights into the dispersal process and the incidence of gene flow on genetic structure (Legrand *et al.*, 2024).

The primary goal of this study is to evaluate the extent to which stepping-stone dispersal, including dispersal across multiple unsampled sites, contributes to the spatial genetic structure of *E. amentacea* in the northwestern Mediterranean Sea. We genotyped 1259 individuals among 43 sites using six microsatellite markers to: (i) assess genetic differentiation among sites and regions, (ii) evaluate the added value of biophysical modelling, which incorporates multi-generation dispersal dynamics and multiple stepping-stone populations, for explaining the genetic structure of *E. amentacea* and (iii) test the hypothesis that long-distance dispersal bypassing intermediate stepping-stones due to habitat discontinuities promotes gene flow between Eastern Provence and Corsica. This study advances our understanding of gene flow dynamics in fragmented marine populations, highlighting the interplay between stepping-stone connectivity and rare long-distance dispersal events.

Material and methods

Model species

Ericaria amentacea has a basal holdfast a few centimetres wide, from which arise dozens of axes up to 40 cm high, which can bear receptacles at their apices.

It forms extensive stands on shallow, wave-exposed rocky substrates. The species has a diploid life cycle strictly involving meiotic sex. Meiosis takes place in hermaphrodite conceptacles clustered within terminal receptacles. Reproduction occurs in late spring and early summer. Fertilization, of an oogamous nature, involves the convergence of thousands of biflagellate male gametes with female gametes near the conceptacles; the zygotes subsequently disperse (Hoek *et al.*, 1995; Susini, 2006). Vegetative reproduction does not occur in this species.

Sampling

Forty-three populations of *E. amentacea* were sampled along the French north-western Mediterranean coast, including Corsica (Fig. 1, Table 1) in spring 2007, 2008 and 2009. Sampling for DNA extraction was carried out by collecting small parts (5–10 cm from the tip) of the secondary branches of each individual, which were then directly dried in silica gel. Individuals were sampled one metre apart to avoid collecting the same individual twice. A total of 1259 individuals, from 30–32 per sampling site, were collected.

Microsatellite genotyping

Dry material (10 mg) from each sample, previously cleaned of epiphytic organisms, was employed for DNA extraction. Genomic DNA was extracted using the DNeasy 96 Plant kit (Qiagen©), and six microsatellites, previously isolated from the species' genome (Robvieux *et al.*, 2012) and selected for their relatively high polymorphism, were employed for characterizing genetic variation. PCR reactions were performed as described in Robvieux *et al.* (2012). Loci M24, M33, M51 and M58 were multiplexed while the two remaining (M35 and M27) were amplified separately. Amplification products were analysed on an ABI 3130 Genetic Analyser. GeneScanTM 600 Liz® Size Standard (0.2 µl) and formamide (10 µl) were added to each well. Allele scoring was performed automatically using STRand v2.4.59 (Toonen & Hughes, 2001). We tested for the presence of null alleles, allele dropout and scoring errors using MICRO-CHECKER v2.2.3 (Van Oosterhout *et al.*, 2004). Samples with missing data were systematically excluded to ensure completeness across all six loci. Linkage disequilibrium was finally tested among all pairs of loci using ARLEQUIN v3.5 with 16 000 permutations (Excoffier *et al.*, 2005).

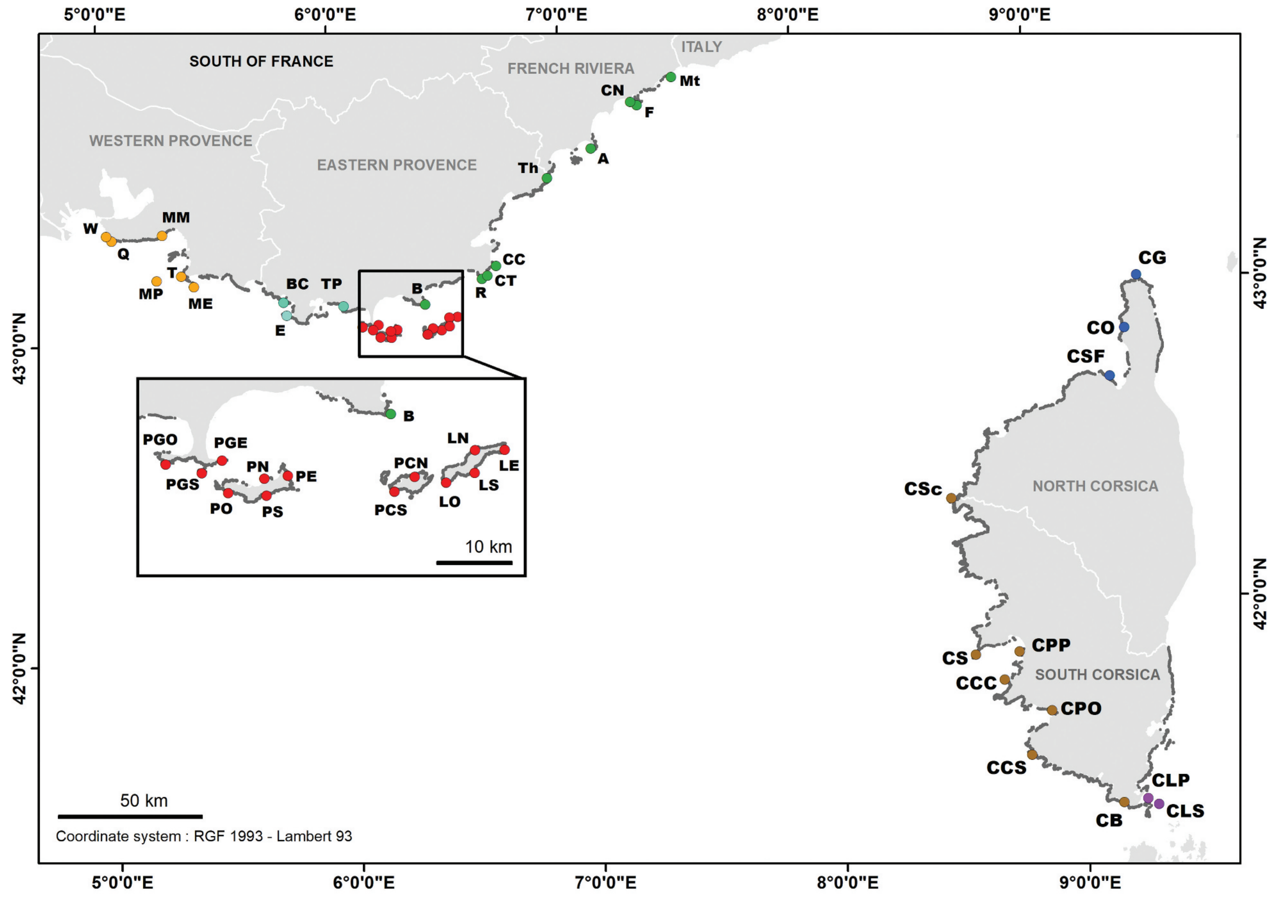

Fig. 1. Geographic positions of the sampled populations of *Ericaria amentacea* are shown. Dot colours represent the delineation of the seven geographic regions.

Table 1. Genetic variation within sampling sites.

Label	Sampling site	Region	n	MLG	Ar	H_e	F_{IS}	P_{val}
W	Martigues	Marseille-Côte Bleue	26	23	2.32	0.41	0.09	0.02
Q	Carro	Marseille-Côte Bleue	26	21	2.36	0.39	0.24	0.00
MM	Mejean	Marseille-Côte Bleue	32	30	2.54	0.39	0.17	0.00
T	Tiboulen	Marseille-Côte Bleue	29	29	2.92	0.40	0.18	0.00
MP	Planier	Marseille-Côte Bleue	25	25	3.17	0.48	0.08	0.00
ME	Empereur	Marseille-Côte Bleue	25	24	3.05	0.45	0.12	0.00
BC	Bandol	Toulon-Bandol	15	14	2.42	0.42	0.36	0.00
E	Embiez	Toulon-Bandol	16	16	2.34	0.43	0.27	0.00
TP	Pradet	Toulon-Bandol	12	12	2.41	0.39	0.06	0.07
PGO	Gien_Ouest	Hyeres Islands	26	26	3.18	0.47	0.07	0.03
PGS	Gien_Sud	Hyeres Islands	25	25	3.65	0.51	0.19	0.00
PGE	Gien_Est	Hyeres Islands	24	23	2.32	0.37	0.15	0.00
PN	Porquerolle_Nord	Hyeres Islands	19	19	3.36	0.49	0.23	0.00
PE	Porquerolle_Est	Hyeres Islands	27	27	2.59	0.42	0.16	0.00
PO	Porquerolle_Ouest	Hyeres Islands	25	25	3.81	0.64	0.12	0.00
PS	Porquerolle_Sud	Hyeres Islands	22	20	2.65	0.36	0.16	0.00
PCS	PCros_Sud	Hyeres Islands	24	23	3.69	0.55	0.15	0.00
PCN	PCros_Nord	Hyeres Islands	19	18	2.34	0.35	0.10	0.27
LN	Levant_Nord	Hyeres Islands	23	21	2.32	0.38	0.00	0.01
LO	Levant_Ouest	Hyeres Islands	25	25	3.29	0.50	0.14	0.00
LS	Levant_Sud	Hyeres Islands	26	25	2.73	0.43	0.12	0.02
LE	Levant_Est	Hyeres Islands	13	12	2.99	0.40	0.18	0.00
B	Bregancon	Eastern Provence	15	15	2.91	0.44	0.16	0.00
R	Lardier	Eastern Provence	23	23	2.90	0.49	0.19	0.00
CT	Taillat	Eastern Provence	28	27	2.27	0.34	0.18	0.00
CC	Camarat	Eastern Provence	28	17	1.83	0.22	−0.02	0.49
Th	Theoule	Eastern Provence	28	27	3.30	0.49	0.13	0.00
A	Antibes	Eastern Provence	23	23	2.93	0.49	−0.02	0.41
CN	Nice	Eastern Provence	27	27	3.51	0.56	0.00	0.11
F	Ferrat	Eastern Provence	27	25	2.64	0.40	0.03	0.34
Mt	Martin	Eastern Provence	9	9	2.81	0.41	0.17	0.01
CG	Giraglia	Cap Corse	32	32	2.76	0.44	0.10	0.01
CCO	Corse_Ouest	Cap Corse	30	26	2.52	0.38	0.01	0.00
CSF	St_Florent	Cap Corse	7	6	1.83	0.21	0.30	0.01
CSc	Scandola	Southwest Corsica	26	26	3.81	0.54	0.16	0.00
CS	Sanguinaires	Southwest Corsica	25	21	2.09	0.29	0.08	0.08
CPP	Porticcio	Southwest Corsica	26	22	2.22	0.31	−0.01	0.38
CCC	Castagna	Southwest Corsica	28	22	2.30	0.38	−0.04	0.29
CPO	Olmetto	Southwest Corsica	32	24	2.19	0.28	0.22	0.00
CCS	Senetosa	Southwest Corsica	42	27	2.75	0.47	0.08	0.04
CB	Bonifacio	Southwest Corsica	30	13	1.63	0.18	0.10	0.10
CLP	Poragia	Southeast Corsica	14	12	2.26	0.28	−0.12	0.82
CLS	Sperduto	Southeast Corsica	17	17	2.66	0.40	−0.03	0.67

n: number of genotyped individuals; MLG: number of multi-locus genotypes; Ar: allelic richness; H_e: expected heterozygosity; F_{IS}: fixation index; Pval: Pvalue from Global Hardy–Weinberg test (Score [U] test) considering the alternative hypothesis of heterozygote deficiency.

Genetic variation

Genetic variation was estimated after correcting the dataset for multilocus genotypes (MLGs) by retaining unique MLGs. MLG identification was performed using the R package Poppr v.2.9.4 (Kamvar *et al.*, 2014, 2015). Within-site genetic variation was assessed by measuring allelic richness, expected heterozygosity (H_e) and F_{IS}, implemented in the R package diveRsity v.1.9.90 (Keenan *et al.*, 2013). Given that positive F_{IS} values have been frequently reported in *Cystoseira* s.l. populations, the Global Hardy–Weinberg test (Score [U] test) (Raymond & Rousset, 1995), implemented in Genepop v. 4.7.5 R package (Rousset, 2008), was used to test departure from panmixia across all loci by considering the alternative hypothesis of heterozygote deficiency. This was accomplished using the Markov chain algorithm (100 000 dememorization steps, 10 000 batches and 10 000 iterations per batch).

Genetic differentiation

Genetic differentiation was inferred among sampling sites and regions (n = 7). In the absence of prior information on the scale and boundaries of genetic regions, regional classification was guided by the spatial genetic structure of the closely related species *E. zosteroides* (Reynes *et al.*, 2021*a*), particularly in our decision to distinguish the Bay of Marseille, Toulon-Bandol and Eastern Provence as separate regions (see Table 1, Fig. 1). The following clusters were defined: from the Côte Bleue to the Bay of Marseille (n = 6 sites), from Toulon to Bandol (n = 3 sites), with a distinction between the Hyères Islands (n = 13 sites) and Eastern Provence (n = 9 sites). The Hyères Islands were treated separately from the continental populations of the Toulon-Bandol region to account for habitat discontinuity due to their insular nature. For Corsica, regional divisions were based on geographic features, given the current lack of genetic data for *Cystoseira* s.l. in this region. Four Corsican regions were defined: the north side (Cap Corse, n = 3 sites), the east side (southeast Corsica, n = 2 sites) and the west side (southwest Corsica, n = 7 sites). An analysis of molecular variance (AMOVA), implemented in Arlequin v.3.11 (Excoffier *et al.*, 2005), was performed with 10 000 permutations to quantify how much of the observed genetic variation is explained by regional differentiation compared with variation among sites or individuals. AMOVA was also performed at the highest clustering level between continental and Corsica populations. Consistent with possible long-distance dispersal events between these regions (Reynes et al., 2021*a*), populations from Eastern Provence were grouped with those from Cap Corse rather than with continental populations to evaluate the proportion of genetic variation explained by this configuration. Between-site differentiation was estimated through pairwise F_{ST} (Nei's G_{st}) and Jost D, both indices implemented in the Mmod 1.3.3 R package (Winter, 2012). An exact test of genic differentiation was conducted (Raymond & Rousset, 1995) with default parameters and completed using the Genepop R package (Rousset, 2008). Finally, an unrooted Neighbour-joining (NJ) tree was built using a dissimilarity distance matrix, implemented in the Poppr R package (Kamvar *et al.*, 2014, 2015). A second NJ tree was built by restricting the dataset to Eastern Provence and Corsica individuals to emphasize finer relationships between Eastern Provence and Cap Corse populations. Support for each node was assessed by performing 100 bootstraps by randomly sampling loci with replacement.

Biophysical modelling

Simulations of oceanographic connectivity were generated with a biophysical modelling framework (Assis *et al.*, 2025). This framework tracks passive Lagrangian particles by integrating daily gridded velocity fields provided by the Copernicus Marine Environment Monitoring Service (CMEMS, https://doi.org/10.48670/moi-00021), a data-assimilative operational ocean model implemented on the global ocean at 1/12° horizontal resolution (approximately 8 km). Connectivity simulations were conducted over the distribution of *E. amentacea*, as inferred by the stacked species distribution model (SDM) provided by Fragkopoulou *et al.* (2022). Particles are released daily from the centres of source sites and collected at sink sites, with both types of sites defined as hexagons with 8.45 km edges, distributed along the coastline throughout the *E. amentacea* range (n = 2,564 source/sink sites). Note that most of the sites were not sampled for genetic analysis and are considered as various potential stepping-stones, or ghost populations, in our framework. The particles were released over 11 years (2010–2020) and advected upon the ocean surface (top vertical layer of the CMEMS model) for up to 180 days until they eventually ended up in sink sites or got lost in the open ocean. We later constructed a matrix assigning the number of particles exchanged between the source site and the sink site, and the associated mean trajectory time in hours.

Ericaria amentacea dispersal capacity

Because there are no reported laboratory/field experiments/observations of the potential duration of the dispersal of *E. amentacea* (e.g. reproductive viability of fragments, raft survival duration, spore settlement rate), we used the global macroalgal dispersal capacity approach summarized in Legrand *et al.* (2024). This method used a dataset of macroalgal dispersal capacity obtained through a literature survey and summarized the information with a normal distribution fitted on sexual dispersal capacity (gametes, zygotes and/or spore release). The probability density function obtained is normalized into a weighting factor function ranging from 0 to 1. Long-distance dispersal events (LDD), promoted by fertile thallus rafting, are considered starting at 33 days (i.e. maximal sexual dispersal capacity, Deysher & Norton, 1981) with a unique weighting factor of 0.01, which corresponds to the proportion of LDD events observed using population assignment tests (D'Aloia *et al.*, 2022). We later weighted, for each sink site, the number of particles incoming for the source site by the weighting factor according to the mean trajectory time.

Multi-generation connectivity and centrality using graph theory

A unique matrix of pairwise probability of connectivity was produced by dividing the weighted number of particles received by sink site from source site by the total weighted number of particles received at sink site, applying the 'backward-in-time' dispersal probability approach in Legrand *et al.* (2022). A square 2564 × 2564 matrix was obtained, summarizing the probability of connectivity among different sink and source sites across the distribution of *E. amentacea*. Graph theory was used to compute asymmetric multi-generation connectivity between all *E. amentacea* sampling populations. We set a graph of 2564 nodes representing the sites, while the edges are indexed by the probabilities of connectivity. The Dijkstra algorithm was used to find the shortest path between sampling sites by minimizing the sum of distance-transformed probabilities (i.e. -log(probabilities); Dijkstra, 1959). Multi-generation connectivity was determined by multiplying edge probabilities along the inferred shortest paths. The number of stepping-stones needed to connect sampling sites was counted, considering each stepping-stone as a site where *E. amentacea* could settle and subsequently disperse again as a new generation. To match the symmetric feature of genetic differentiation, the anisotropic multi-generation probability was transformed between pairs of sampling sites to a symmetric probability with $P = P_{AB} + P_{BA} - P_{AB}P_{BA}$ (Legrand *et al.*, 2022, 2024). Note that the average pairwise genetic differentiation levels were computed when two or more sampled populations were found within a site. In addition, a centrality graph-based index was used to assess the potential role of centrality in population connectivity (Gouvêa *et al.*, 2023; Legrand *et al.*, 2024). The harmonic centrality metric was considered, which calculates, for each node, the inverse of the total length of the shortest paths between that node and all other nodes (Marchiori & Latora, 2000). This metric is similar to the closeness centrality (Gouvêa *et al.*, 2023), but it accommodates non-connected graphs, which applies to our case.

Seascape genetic analysis

Global and partial distance-based redundancy analyses (db-RDA, Legendre & Anderson, 1999) were performed to evaluate the separate and joint effects of coastal distance and oceanographic connectivity on spatial genetic differentiation. Individual coordinates of principal coordinate analysis (PCoA) based on Jost's D matrix (see genetic differentiation section) were used as the response variable. Jost's D, instead of F_{ST}, can be more suitable when considering populations with different levels of genetic diversity (Whitlock, 2011), as suggested in our study. Coastal distance and probability of connectivity from biophysical modelling were respectively transformed into distance-based Moran's eigenvector maps (or dbMEM, Dray *et al.*, 2006) and Asymmetric Eigenvector Maps (or AEM, Blanchet *et al.*, 2008) following the method described in Fouqueau *et al.* (2024). Given the extensive horizontal resolution of the biophysical model, sampling sites belonging to the same model source/sink site receive the same dispersal probabilities. Variable selection was conducted through a stepwise forward process using the ordiR2step function from the 'vegan' R package (Oksanen, 2010). This function identifies variables to construct the most effective model, defined as the model that maximizes the adjusted coefficient of determination (R^2_{adj}) while minimizing the P (Blanchet *et al.*, 2008). Subsequently, an analysis of variance (ANOVAs; 1000 permutations) was executed to evaluate the significance of the model, axes and the selected variables.

Results

Genetic variation

Among the six microsatellite loci considered, five showed high polymorphic information content (PIC) values (ranging from 0.44–0.88), with 10–20 distinct alleles per locus. Only locus M24 showed relatively low polymorphism, with five distinct alleles and a PIC value of 0.28 (Supplementary table S1). Nevertheless, the regional patterns of differentiation highlighted by the PCA based on individual genotypes support interest in these markers for addressing our research questions (Supplementary fig. S1). Analyses of pairwise independence between loci ('linkage equilibrium') indicated that the six microsatellites were independent of each other after performing FDR correction ($p < 0.05$). Null alleles were not detected according to MICRO-CHECKER outputs; therefore, the six microsatellites were used for the subsequent analyses of genetic variation. Among the 1021 genotyped and quality-filtered samples, 912 unique multilocus genotypes (MLGs) were identified. Given that repeated MLGs can bias F-statistics (e.g. Halkett *et al.*, 2005; Krueger-Hadfield *et al.*, 2011; Reynes *et al.*, 2021*b*), they were removed from subsequent analyses of genetic variation. However, we acknowledge that repeated MLGs observed here likely reflect the extent of selfing within populations, random association of alleles by chance due to the small number of markers used, rather than clonal reproduction. In this corrected dataset, significant heterozygote deficiency ($p < 0.05$, overall U test), with F_{IS} ranging from −0.12 to 0.36,

Table 2. Genetic variation within sampling sites at the regional level. Parameters are average across sites within the same region, and values in parentheses indicate the range among sites for each parameter.

Region	Ar	H_e	F_{IS}	Ratio P_{val}
Marseille-Côte Bleue	2.73 (2.32–3.17)	0.42 (0.39–0.48)	0.08–0.24	1.00
Toulon-Bandol	2.39 (2.34–2.42)	0.41 (0.39–0.43)	0.06–0.36	0.67
Hyeres Islands	2.99 (2.32–3.81)	0.45 (0.35–0.64)	0-0.23	0.92
Eastern Provence	2.79 (1.83–3.51)	0.43 (0.22–0.56)	−0.02–0.19	0.56
Cap Corse	2.37 (1.83–2.76)	0.34 (0.21–0.44)	0.01–0.3	1.00
Southeast Corsica	2.46 (2.26–2.66)	0.34 (0.28–0.40)	−0.12–0.03	0.00
Southwest Corsica	2.43 (1.63–3.81)	0.35 (0.18–0.54)	−0.04–0.22	0.43

Ar: allelic richness; H_e: expected heterozygosity; F_{IS}: fixation index; RatioP_{val}: ratio of sampling sites showing a significant heterozygote deficiency.

was reported among 32 out of the 43 sampling sites. Differences in within-site genetic variation were reported among the studied regions, with He of 0.34–0.35 (average among sites of the same region) in the Corsican regions, in contrast to He of 0.41–0.45 in continental regions (Table 2). The proportion of sampling sites showing a significant heterozygote deficiency ($p < 0.05$, overall U test) ranged from 0.56 in Eastern Provence to 1 in both Marseille-Côte Bleue and Cap Corse populations (Table 2). The lowest level of genetic variation was reported in Southwest Corsica at CB (H_e = 0.18, ar = 1.63). The genetic parameters evaluated (i.e. allelic richness (ar), expected heterozygosity (H_e) and F_{IS}) are also provided per site (Table 1).

Genetic differentiation

The average F_{ST} and Jost's D values were equal to 0.34 and 0.39, respectively. Pairwise F_{ST} ranged from 0.04–0.43, and pairwise Jost's D from 0.03–0.83. Highest differentiation was reported for pairwise comparisons with Théoule-sur-Mer (Th) and Antibes (A), both located in the Eastern Provence region (Supplementary fig. S2). The exact test of genic differentiation yielded significant results ($p < 0.001$) for all 903 pairwise-site comparisons. AMOVA revealed that most of the genetic variation was attributable to within-site variance (64%, $p < 0.001$), followed by variation among sites within the same region (25%, $p < 0.001$), and finally by variation among regions (11%, $p < 0.001$; Table 3). The second AMOVA revealed that assigning Eastern Provence to the North Corsica region reduced the genetic variation between continental and Corsican populations to 28%, compared with 31% when Eastern Provence was grouped with the continental cluster (Table 3).

At the regional level, genetic differentiation between Eastern Provence and the Cap Corse populations was moderate (F_{ST} = 0.04; Jost's D = 0.11) compared with, for instance, between Marseille-Côte Bleue and Eastern Provence clusters (F_{ST} = 0.10; Jost's D = 0.31, Fig. 2). The Neighbour-Joining tree displayed multiple basal branches and several clusters, emphasizing the uniqueness of populations from Marseille-Côte Bleue (dark blue, Fig. 3a), which cluster separately from other continental and Corsican populations distributed across several groups. Performing the Neighbour-Joining analysis restricted to Eastern Provence and Corsica populations highlighted the close relationship between Cap Corse and several Eastern Provence populations (i.e. CN, F, MT). Most Cap Corse individuals clustered with the Eastern Provence region rather than with other Corsican populations (Fig. 3b).

Oceanographic connectivity

The biophysical model showed that all sampling sites of *E. amentacea* are potentially interconnected, forming a network of 153 connections in total. Among them, 29% of the connections are directly completed through a single generation. This primarily occurs between neighbouring populations (e.g. the populations of the Hyères Islands, as depicted in the below-diagonal elements of Fig. 4a) and, due to rafting events that facilitate long-distance dispersal, between Corsican populations and some continental populations (i.e. Eastern Provence, Hyères Islands and Toulon-Bandol). The remaining populations are connected through 2–8 generations across multiple unsampled sites acting as stepping-stones, considering a generation as *E. amentacea* settling in a stepping-stone site and dispersing again after reproduction (via gamete, zygote and/or spore release) or through thallus detachment and rafting. The easterly populations of Provence (i.e. Th, A, CN and F) connect the populations of the Hyères Islands and Toulon-Bandol within 3–5 generations, as well as

Table 3. Analyses of molecular variance (AMOVA) considering seven regions as detailed in Table 1, comparing continent versus Cap Corse versus South Corsica. AMOVA were performed both including and excluding the Eastern Provence populations of the Cap Corse cluster.

Source of variation	D.f	Sum of Squares	Var. components	Variation (%)	p value
Seven regions					
Among regions	6	4834	0.21	10.7	<0.001
Among sites within the same region	36	889	0.49	25.4	<0.001
Within sites	1999	2481	1.24	63.9	<0.001
Continent vs Cap Corse (excl. Eastern Provence) vs South Corsica					
Among regions	2	190	0.13	6.7	<0.001
Among sampling sites within the same region	40	1183	0.60	30.5	<0.001
Within sites	1999	2481	1.24	62.8	<0.001
Continent vs Cap Corse (incl. Eastern Provence) vs South Corsica					
Among regions	2	276	0.17	8.5	<0.001
Among sampling sites within the same region	40	1097	0.55	28.29	<0.001
Within sites	1999	2481	1.24	63.1	<0.001

	Marseille−Cbleue	Toulon−Bandol	Hyeres islands	Eastern Provence	Corsican cape	Southeast Corsica	Southwest Corsica
Marseille−Cbleue		0.1	0.07	0.1	0.11	0.16	0.11
Toulon−Bandol	0.27		0.04	0.07	0.09	0.16	0.11
Hyeres islands	0.21	0.14		0.04	0.05	0.11	0.07
Eastern Provence	0.31	0.22	0.15		0.04	0.12	0.1
Corsican cape	0.25	0.21	0.13	0.11		0.13	0.08
Southeast Corsica	0.32	0.37	0.27	0.28	0.22		0.12
Southwest Corsica	0.25	0.27	0.19	0.29	0.16	0.21	

Fig. 2. Heatmap of pairwise F_{ST} (above the diagonal) and Jost's D (below the diagonal) averaged among sampling sites at the regional level. Cold colours indicate low to moderate levels of genetic differentiation, while warm colours indicate high genetic differentiation.

Marseille-Côte Bleue with the southern Corsican populations (greater than the 0.75 interquartile). Despite their close geographic proximity, populations of the Cap Corse and CSc, Cs and CPP populations of Southwest Corsica require 6–8 generations to connect.

Regarding the probability of connections, neighbouring populations are the most likely connected, as represented by the red element above the diagonal of the connectivity matrix in Fig. 4a (i.e. extreme values with a probability > 0.027). Corsican populations are generally isolated from continental populations, with probabilities mostly falling in the lowest 25th percentile (blue elements in the upper triangle of the matrix, Fig. 4a). However, the three populations of the Cap Corse, and at a certain point CSc, appear to be more connected to continental populations, particularly those of the Hyères Islands and Eastern Provence (PE, PCS, PCN, LO, LN, LS, LE, B, R, CT, CC, Th and A). These Cap Corse populations are also less connected to southern Corsican populations. The continental range populations (e.g. W, Q, MM and T in the Marseille-Côte Bleue group and Mt in the Eastern Provence group) are the least connected to other continental populations, with probabilities below the 0.75 interquartile (yellow elements in Fig. 4).

Seascape analyses

When partitioning the effects of coastal distance and oceanographic connectivity on genetic differentiation

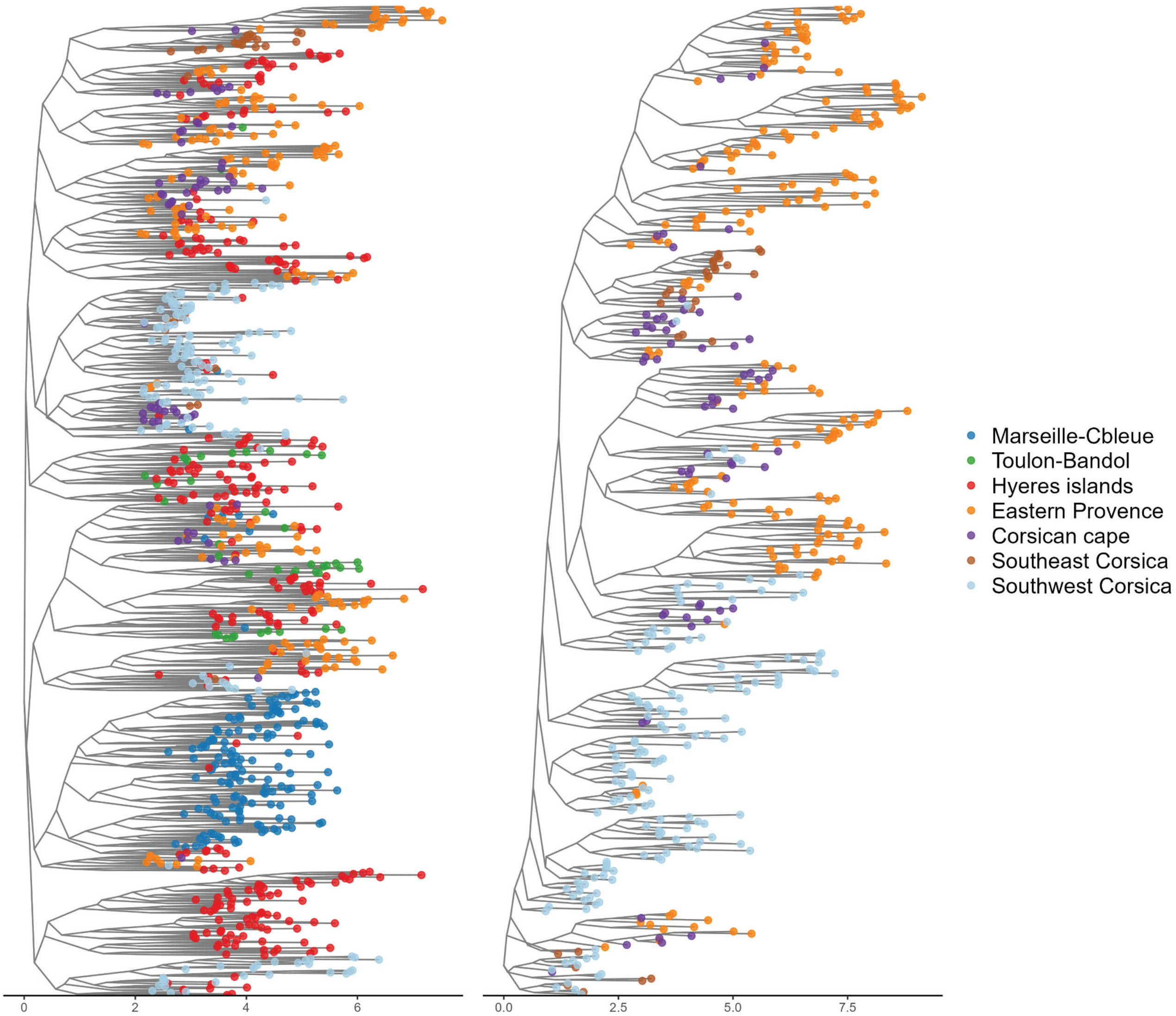

Fig. 3. Unrooted phylogenetic tree built using the Neighbour-Joining (NJ) method. The left panel displays all sampling sites, while the right panel focuses on populations from Eastern Provence and Corsica.

using partial db-RDA, both models were significant ($p < 0.001$). The partial db-RDA accounting for geographic distance selected two predictors (MEM-1, MEM-2; $p < 0.001$) and yielded an adjusted R^2 of 0.13. The partial db-RDA accounting for oceanographic connectivity highlighted four predictors (AEM-1, AEM-14, AEM-11 and AEM-10; $p < 0.001$) and resulted in an adjusted R^2 of 0.19 (Supplementary table S2; for partial db-RDA biplots, see Supplementary figs S3 and S4). The global db-RDA model, accounting for both MEM and AEM predictors, selected in the partial db-RDA was also significant ($p < 0.001$) with $R^2_{adj} = 0.23$. Among the four AEMs, AEM-1, AEM-14 and AEM-11 were conserved in the global model, along with MEM-1 and MEM-2. The first two axes, accounting for 45% and 36% of the variance, respectively, were significant ($p < 0.001$). The first RDA axis primarily separates Marseille-Côte Bleue from the other regions (Fig. 5). This axis is mainly driven by MEM-2, AEM-11 and AEM-14, which exhibit strong differentiation in their vector values between Marseille-Côte Bleue and the other regions (Figs 6 and 7). The second RDA axis primarily differentiates Corsican populations from those on the continent. While this distinction is explained mainly by geography (i.e. MEM-1), differentiation between the two regions is partial when considering oceanographic connectivity (i.e. AEM-1). Notably, Cap Corse populations and those at the eastern limit of Eastern Provence are poorly differentiated in the db-RDA and exhibit similar values along the AEM-1 vector (Fig. 7), highlighting the potential connectivity between these two regions.

Discussion

This study represents the first large-scale investigation of genetic variation in *E. amentacea* across the north-western Mediterranean Sea. Microsatellite-based analyses revealed that all tested sites are genetically differentiated from each other, despite evidence of extensive dispersal among populations. Multi-

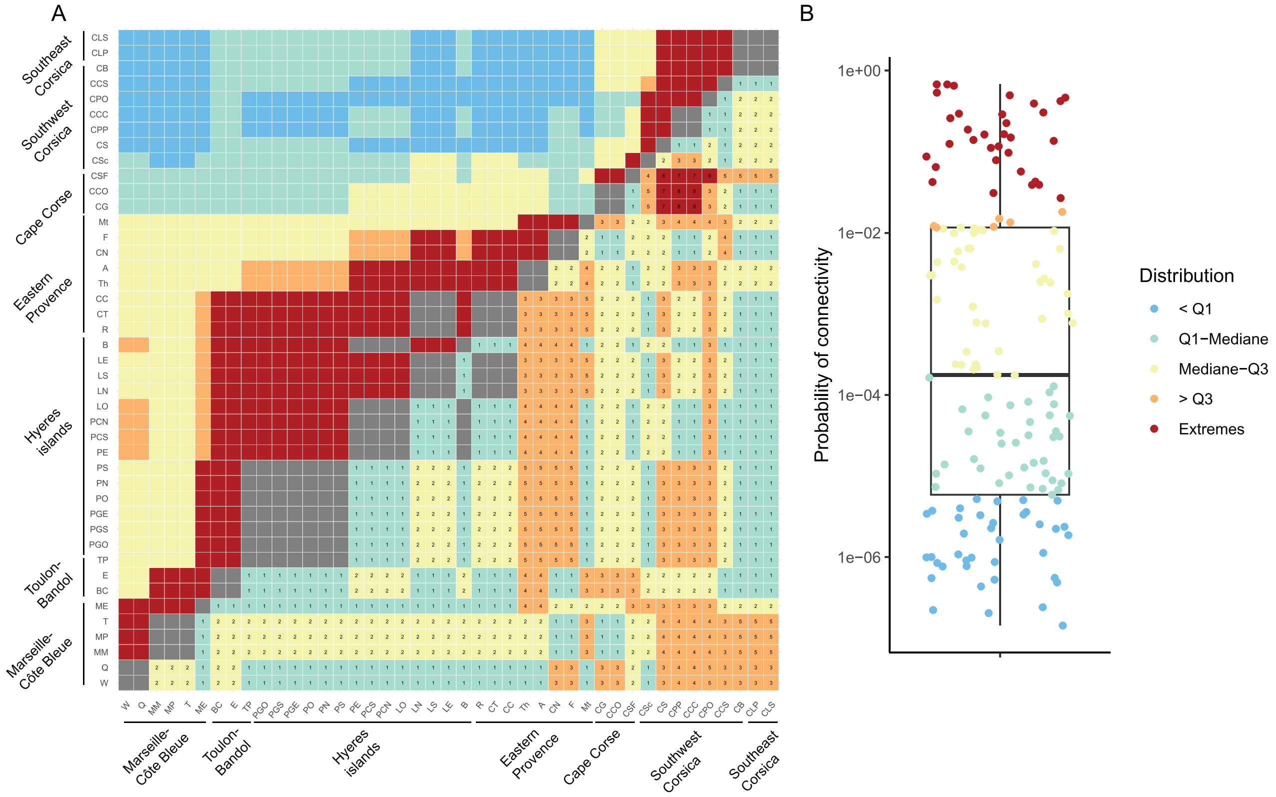

Fig. 4. Oceanographic connectivity of *Ericaria amentacea*. Panel A depicts the connectivity matrix, with the upper panel showing the probability of connectivity and the lower panel indicating the number of generations needed to connect the populations. Panel B displays the distribution of probability of connectivity, which is reported on the connectivity matrix.

generation dispersal estimates, incorporating distribution-based potential stepping-stone populations, uncovered regional connectivity patterns and their role in shaping the genetic structure of *E. amentacea*.

AMOVA indicated that genetic variation occurs primarily between individuals, suggesting that genetic differentiation may be effective at fine spatial scales (10–100 m), probably due to short dispersal distances and selfing, maintaining partially restricted mating. This finding is consistent with previous studies reporting within-site variation (71%) (Susini *et al.*, 2007) and significant fine-scale differentiation across 10-m transects in this species (Buonomo *et al.*, 2017). Partially restricted mating and selfing are further supported by significant heterozygote deficits observed in 32 of the studied populations, consistent with patterns of genetic variation in *Cystoseira* s.l. species (Thibaut *et al.*, 2016; Buonomo *et al.*, 2017, 2018; Bermejo *et al.*, 2018; Riquet *et al.*, 2021; Reynes *et al.*, 2021*a*).

Restricted mating may be driven by the relatively large size of the zygote (100 μm) and its short lifespan before fixation (Susini, 2006; Mangialajo *et al.*, 2012), which limit dispersal and reduce homogeneous gamete mixing within a sampling unit. This subdivision of the population into small breeding groups implies that genetic drift plays a significant role in driving fine-scale differentiation (Li & Hedgecock, 1998). Differentiation can be further accentuated by temporal effects, where the mixing of different cohorts co-occurring within a sampling unit generates temporal genetic differentiation. This is closely related to the strength of genetic drift and variance in reproductive success (Ryman, 1997; Broquet *et al.*, 2013), which influence changes in allele frequencies between generations. Such a cohort structure is well-documented in *Cystoseira* s.l. species (e.g. Ballesteros, 1990; Ballesteros *et al.*, 2009; Robvieux, 2013; Capdevila *et al.*, 2015) and results in patterns of differentiation both between overlapping generations in the red coral (Ledoux *et al.*, 2010) and between discrete generations in the brown alga *Laminaria digitata* (Reynes *et al.*, 2024). Additionally, differentiated cohorts may also arise from high variance in dispersal, mainly when they consist of offspring from genetically distinct populations.

This study emphasizes that genetic differentiation was significant among all sampling sites, including all 903 pairwise comparisons, even those involving short distances between sites (~2.5 km). Oceanographic connectivity remains the most significant factor explaining the genetic structure of E. amentacea, at the large scale of the northwestern Mediterranean Sea (present study), at a comparable scale in southern Italy (Buonomo *et al.*, 2017), and even within more restricted areas such as the Bay of Marseille (Thibaut *et al.*, 2016). More broadly, oceanographic connectivity has often been identified as a key predictor of

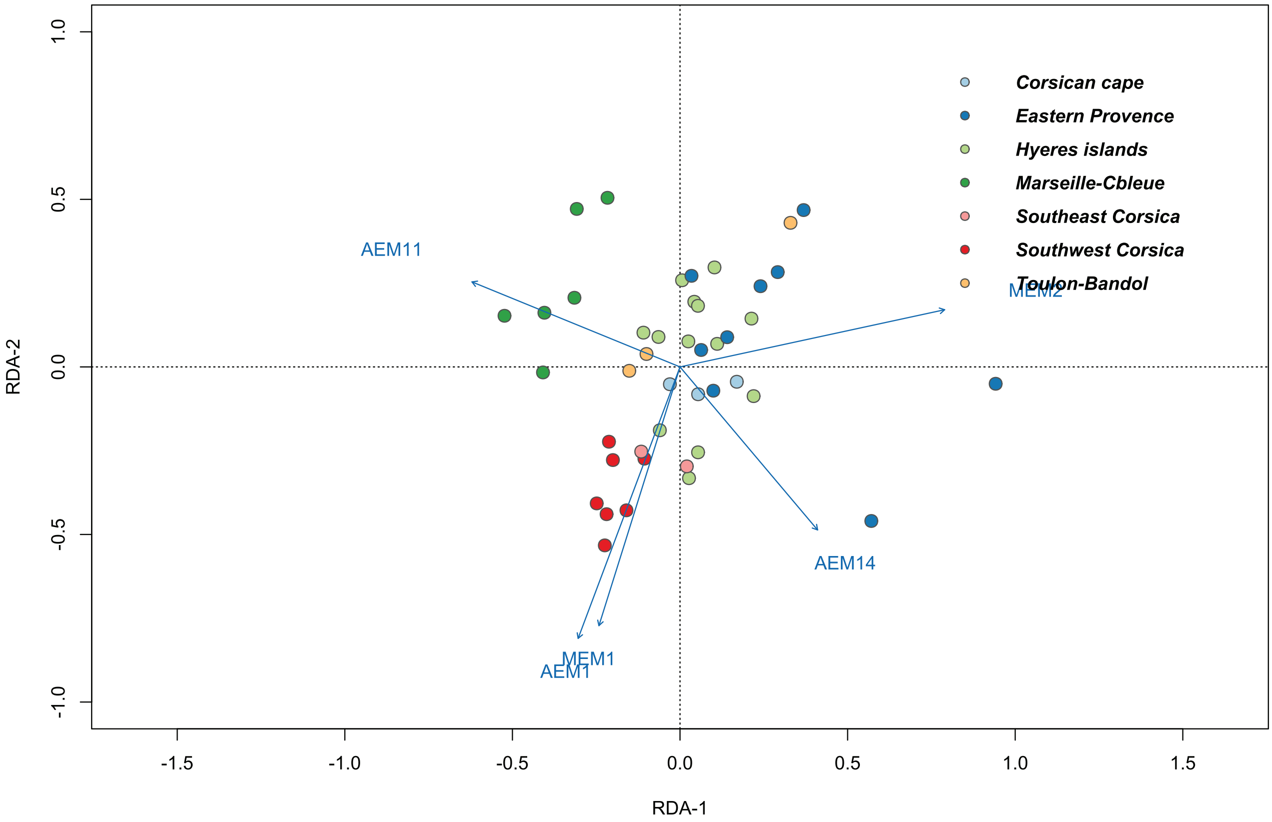

Fig. 5. Axes 1 and 2 of the global db-RDA biplot. Colours represent the seven geographic regions defined in Table 1. Blue arrows indicate the relative contributions of oceanographic connectivity (Asymmetric Eigenvector Maps; AEM) and coastal distances (Moran's Eigenvector Maps; MEM) to genetic variation, as identified through ANOVA and stepwise forward selection (ordiR2step). Arrow length reflects the strength of each predictor's contribution.

genetic structure in kelp and seaweed (e.g., Alberto *et al.*, 2011; Assis *et al.*, 2018, 2021, 2022), although its relative contribution may vary depending on the sampling scheme (Dalongeville *et al.*, 2018; Fouqueau *et al.*, 2024). The role of oceanographic connectivity in facilitating occasional gene flow between geographically distant populations is also mirrored in the low to moderate genetic differentiation observed among such regions. For instance, the moderate differentiation between North Corsica and Eastern Provence populations appears to be primarily driven by oceanographic connectivity, as indicated by the db-RDA model. In this case, long-distance dispersal may occur within a single generation, likely via the transport of floating rafts carrying fertile thalli. In contrast, across shorter spatial scales, gene flow seems to be more strongly supported by multi-generation dispersal. For example, 3–5 generations would be required to connect populations in Eastern Provence with those in the Hyères Islands.

Oceanographic connectivity estimates indicate that dispersal, particularly between neighbouring populations, is relatively frequent, yet populations remain moderately to highly genetically differentiated. This apparent discordance is not unique to the present study; it has also been observed in other *Cystoseira* species, where genetic differentiation persists despite evidence of efficient dispersal potential (Thibaut *et al.*, 2016; Buonomo *et al.*, 2017), and even in other brown algae (e.g., Fouqueau *et al.*, 2024). This dichotomy highlights that gene flow may be restricted despite dispersal mediated by ocean currents. Several non-exclusive processes may explain this pattern. One explanation relates to the technical limitations of the study. For instance, the spatial resolution of the velocity fields used in the biophysical model (i.e. 1/12°, which is ~9 km in those latitudes), as well as the source/sink sites resolution (i.e. 8.45 km hexagons' edge), limits the model's ability to resolve fine-scale dispersal patterns occurring along complex coastal topographies. At this scale, barriers to connectivity operating within a single site would go undetected. Similarly, the relatively limited number of genetic markers may constrain our ability to detect fine-scale genetic structure, although microsatellites can be as informative as thousands of biallelic SNPs for inferring genetic structure due to their high polymorphism and multi-allelic nature (e.g. Guzinski *et al.*, 2018). Another explanation relates that gene flow across heterogeneous environments may be impeded by differential selection, which favours locally adapted alleles (Johnson & Black, 1982). For example, specific genetic variants may be better suited to high wave exposure, desiccation, or

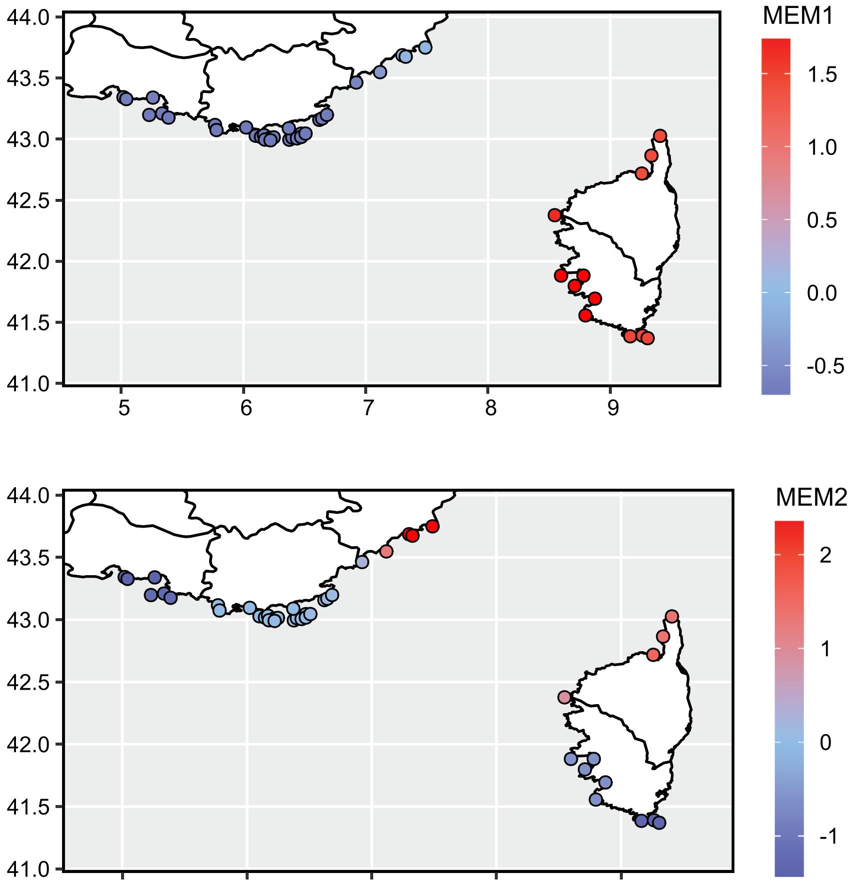

Fig. 6. Spatial representation of Moran's Eigenvector Maps (MEM-1 and MEM-2), with similar colours representing similar MEM values.

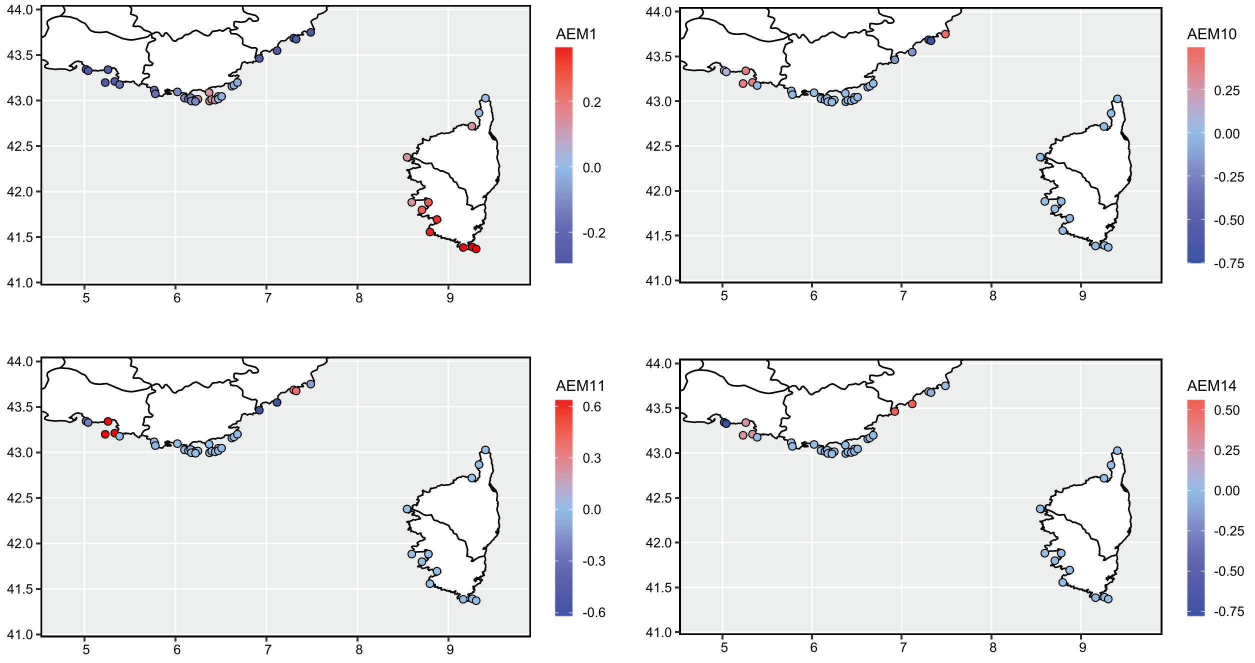

Fig. 7. Spatial representation of Asymmetric Eigenvector Maps (AEM-1, AEM-10, AEM-11 and AEM-14), with similar colours representing similar AEM values.

environments with high predation pressure, potentially constraining gene flow and maintaining differentiation in genomic regions involved in these selective processes. Genomic signatures of local adaptation have already been pinpointed in other brown macroalgae (e.g. Guzinski *et al.*, 2020; Vranken *et al.*, 2021; Reynes *et al.*, 2024); nonetheless, specifically testing the impact of divergent selection on gene flow in *Cystoseira* s.l. will require extensive genome coverage (e.g. genome-wide SNPs; Reynes *et al.*, 2021*a*), supported by dedicated genomic resources and optimized sampling strategies.

Beyond this selective perspective, local habitats may reach their maximum carrying capacity, thereby limiting the successful settlement of *E. amentacea* migrants (Del Monte-Luna *et al.*, 2004). In this scenario, migrant zygotes can also become diluted within the local gene pool, forming density barriers that inhibit or even prevent gene flow while the dispersal process is successful (De Meester *et al.*, 2002). This is also known as the priority effect (De Meester *et al.*, 2002) and has been proposed to explain the strong genetic structure of fucoids (e.g. Neiva *et al.*, 2012; Thibaut *et al.*, 2016; Reynes *et al.*, 2021*a*). Moreover, the recruitment efficiency of *Cystoseira* species could be hampered by ocean warming and acidification (Monserrat *et al.*, 2022), potentially reducing the effectiveness of multi-generation connectivity across stepping-stones. Indeed, the spatio-temporal variability of the different ecological processes related to an accurate connectivity event – settlement, recruitment, reproduction (Pineda *et al.*, 2007) – combined with demographic processes such as the priority effect, is expected to trigger or prevent gene flow across the stepping-stone populations. Considering this potential variability in the further development of the multi-generation models of connectivity (Kool *et al.*, 2010) could be crucial for assessing gene flow more accurately and better understanding the observed patterns of genetic differentiation.

Overall, our results underscore the pivotal role of dispersal over multiple generations and across various stepping-stones in shaping the genetic structure of *E. amentacea*, a canopy-forming species with limited dispersal potential. These insights can support the design of spatially effective conservation strategies aimed at preserving the evolutionary potential, local adaptation and resilience of this keystone marine species, particularly by emphasizing the connectivity networks among populations and identifying sites that contribute disproportionately to gene flow.

Acknowledgements

This project was funded by the MARFOR Biodiversa/0004/2015 project. The project leading to this publication has received funding from the European FEDER Fund under project 1166-39417.

Author contributions

TT, RL and BL developed the main conceptual ideas and performed field sampling with BA. RL analysed the genetic data and their association with the dispersal model. RL wrote the manuscript with LT, who was also in charge of oceanographic modelling and dispersal inferences. All authors provided critical feedback and were fully involved in the revision process.

Disclosure statement

No potential conflict of interest was reported by the author(s).

Data availability statement

The pipeline of the biophysical model used to estimate oceanographic connectivity can be accessed at https://github.com/TerenceLegrand/connectivity_of_marine_forests. All microsatellite datasets and associated metadata used in this study are publicly available at Figshare: https://doi.org/10.6084/m9.figshare.29367773.v1.

Supplementary material

The following supplementary material is accessible via the Supplementary Content tab on the article's online page at https://doi.org/10.1080/09670262.2025.2554068

Supplementary table S1. Per-locus genetic variation, including the number of different alleles (Na), heterozygosity (H), and Polymorphism Information Content (PIC), is reported.

Supplementary table S2. Results of the partial and global db-RDA. Oceanographic connectivity and Coastal distance predictors selected by the stepwise forward selection (ordiR2step). The predictors highlighted in bold are significant at $p < 0.001$ using ANOVA. The adjusted coefficient of determination (R2 adj) and the p-value of the model are reported.

Supplementary fig. S1. Principal Component Analysis (PCA) of individual genotypes, showing PC1, PC2, PC3, and PC4. Samples are color-coded by assigned region.

Supplementary fig. S2. Heatmap of pairwise FST (above the diagonal) and Jost's D (below the diagonal) between sampling sites. Cold colors indicate low to moderate levels of genetic differentiation, while warm colors indicate high genetic differentiation.

Supplementary fig. S3. Partial db-RDA biplot accounting for coastal distance

Supplementary fig. S4. Partial db-RDA biplot accounting for oceanographic connectivity

References

Alberto, F., Raimondi, P.T., Reed, D.C., Watson, J.R., Siegel, D.A., Mitarai, S. & Serrao, E.A. (2011). Isolation by oceanographic distance explains genetic structure for *Macrocystis pyrifera* in the Santa Barbara Channel. *Molecular Ecology*, **20**(**12**): 2543–2554.

Assis, J., Failler, P., Fragkopoulou, E., Abecasis, D., Touron-Gardic, G., Regalla, A., Sidina, E., Dinis, H. & Serrao, E.A. (2021). Potential biodiversity connectivity in the network of marine protected areas in Western Africa. *Frontiers In Marine Science*, **8**: 765053.

Assis, J., Fragkopoulou, E., Serrão, E.A. & Araújo, M.B. (2025). Coastal oceanographic connectivity at the global scale: a dataset of pairwise probabilities and travel times derived from biophysical modeling. *Scientific Data*, **12**(**1**): 737.

Assis, J., Neiva, J., Bolton, J.J., Rothman, M.D., Gouveia, L., Paulino, C., Mohdnasir, H., Anderson, R.J., Reddy, M. M., Kandjengo, L., Kreiner, A., Pearson, G.A. & Serrão, E.A. (2022). Ocean currents shape the genetic structure of a kelp in southwestern Africa. *Journal of Biogeography*, **49**(**5**): 822–835.

Assis, J., Serrão, E.Á., Coelho, N.C., Tempera, F., Valero, M. & Alberto, F. (2018). Past climate changes and strong oceanographic barriers structured low-latitude genetic relics for the golden kelp *Laminaria ochroleuca*. *Journal of Biogeography*, **45**(**10**): 2326–2336.

Ballesteros, E. (1990). Structure and dynamics of the community of *Cystoseira* C.Agardh. *Scientia Marina*, **54**: 217–229.

Ballesteros, E., Garrabou, J., Hereu, B., Zabala, M., Cebrian, E. & Sala, E. (2009). Deep-water stands of *Cystoseira zosteroides* C.Agardh (Fucales, Ochrophyta) in the Northwestern Mediterranean: insights into assemblage structure and population dynamics. *Estuarine, Coastal and Shelf Science*, **82**(**3**): 477–484.

Bermejo, R., Chefaoui, R.M., Engelen, A.H., Buonomo, R., Neiva, J., Ferreira-Costa, J., Pearson, G.A., Marba, N., Duarte, C.M., Airoldi, L., Hernandez, I., Guiry, M.D. & Serrão, E.A. (2018). Marine forests of the Mediterranean-Atlantic *Cystoseira tamariscifolia* complex show a southern Iberian genetic hotspot and no reproductive isolation in parapatry. *Scientific Reports*, **8** (**1**): 10427.

Blanchet, F.G., Legendre, P. & Borcard, D. (2008). Modelling directional spatial processes in ecological data. *Ecological Modelling*, **215**(**4**): 325–336.

Blanfuné, A., Boudouresque, C.F., Verlaque, M., Beqiraj, S., Kashta, L., Nasto, I., Ruci, S. & Thibaut, T. (2016a). Response of rocky shore communities to anthropogenic pressures in Albania (Mediterranean Sea): ecological status assessment through the CARLIT method. *Marine Pollution Bulletin*, **109**: 409–418.

Blanfuné A., Boudouresque, C.F., Verlaque, M., Thibaut, T., (2016b). The fate of *Cystoseira crinita*, a forest-forming Fucale (Phaeophyceae, Stramenopiles), in France (North Western Mediterranean Sea). *Estuarine, Coastal and Shelf Science*, **181**: 196–208.

Blanfuné, A., Boudouresque, C.F., Verlaque, M. & Thibaut, T. (2019). The ups and downs of a canopy-forming seaweed over a span of more than one century. *Scientific Reports*, **9**: 5250.

Blanfuné, A., Thibaut, T., Boudouresque, C.F., Mačić, V., Markovic, L., Palomba, L., Verlaque, M. & Boissery, P. (2017). The CARLIT method for the assessment of the ecological quality of European Mediterranean waters: relevance, robustness and possible improvements. *Ecological Indicators*, **72**: 249–259.

Blanfuné, A., Verlaque, M., Boudouresque, C.F., Rozis, E. & Thibaut, T. (2022). *Les Forêts Marines De France Et De Méditerranée: Guide De Détermination Des Espèces-Ingénieurs (Sargassaceae, Fucales, Phaeophyceae)*. Presse Universitaire de Provence, Aix-en-Provence (Bouches-du-Rhône).

Broquet, T., Viard, F. & Yearsley, J.M. (2013). Genetic drift and collective dispersal can result in chaotic genetic patchiness. *Evolution*, **67**(**6**): 1660–1675.

Bruno de Sousa, C., Cox, C.J., Brito, L., Pavão, M.M., Pereira, H., Ferreira, A., Ginga, C., Campino, L., Bermejo, R., Parente, M. & Varela, J. (2019). Improved phylogeny of brown algae *Cystoseira* (Fucales) from the Atlantic-Mediterranean region based on mitochondrial sequences. *PLOS ONE*, **14**(**1**): e0210143.

Buonomo, R., Assis, J., Fernandes, F., Airoldi, L., Engelen, A.H. & Serrao, E.A. (2017). Habitat continuity and stepping-stone oceanographic distances explain population genetic connectivity of the brown alga *Cystoseira amentacea*. *Molecular Ecology*, **26**: 766–780.

Buonomo, R., Chefaoui, R.M., Lacida, R.B., Engelen, A.H., Serrão, E.A. & Airoldi, L. (2018). Predicted extinction of unique genetic diversity in marine forests of *Cystoseira* spp. *Marine Environmental Research*, **138**: 119–128.

Capdevila, P., Linares, C., Aspillaga, E., Navarro, L., Kersting, D.K. & Hereu, B. (2015). Recruitment patterns in the Mediterranean deep-water alga *Cystoseira zosteroides*. *Marine Biology*, **162**: 1165–1174.

Capdevila, P., Linares, C., Aspillaga, E., Riera, J.L. & Hereu, B. (2018). Effective dispersal and density-dependence in mesophotic macroalgal forests: insights from the Mediterranean species *Cystoseira zosteroides*. *PLOS ONE*, **13**(**1**): e0191346.

Coleman, M.A. & Kelaher, B.P. (2009). Connectivity among fragmented populations of a habitat-forming alga, *Phyllospora comosa* (Phaeophyceae, Fucales) on an urbanised coast. *Marine Ecology Progress Series*, **381**: 63–70.

Couceiro, L., Robuchon, M., Destombe, C. & Valero, M. (2013). Management and conservation of the kelp species *Laminaria digitata*: using genetic tools to explore the potential exporting role of the MPA "Parc naturel marin d'Iroise". *Aquatic Living Resources*, **26**(**2**): 197–205.

D'Aloia, C.C., Bogdanowicz, S.M., Andrés, J.A. & Buston, P.M. (2022). Population assignment tests uncover rare long-distance marine larval dispersal events. *Ecology*, **103**(**1**): c03559.

Dalongeville, A., Andrello, M., Mouillot, D., Lobreaux, S., Fortin, M.J., Lasram, F., Belmaker, J., Rocklin, D. & Manel, S. (2018). Geographic isolation and larval dispersal shape seascape genetic patterns differently according to spatial scale. *Evolutionary Applications*, **11**(**8**): 1437–1447.

DEl Monte-Luna, P., Brook, B.W., Zetina-Rejón, M.J. & Cruz-Escalona, V.H. (2004). The carrying capacity of ecosystems. *Global Ecology and Biogeography*, **13**(**6**): 485–495.

De Meester, L., Gómez, A., Okamura, B. & Schwenk, K. (2002). The Monopolization Hypothesis and the dispersal–gene flow paradox in aquatic organisms. *Acta Oecologica*, **23**(**3**): 121–135.

Devescovi, M. & Ivesa, L. (2007). Short term impact of planktonic mucilage aggregates on macrobenthos along the Istrian rocky coast (Northern Adriatic, Croatia). *Marine Pollution Bulletin*, **54**: 887–893.

Deysher, L. & Norton, T.A. (1981). Dispersal and colonization in *Sargassum muticum* (Yendo) Fensholt. *Journal of Experimental Marine Biology and Ecology*, **56**(**2–3**): 179–195.

Dijkstra, E.W. (1959). A note on two problems in connexion with graphs. *Numerische Mathematik*, **1**(**1**): 269–271.

Dray, S., Legendre, P. & Peres-Neto, P.R. (2006). Spatial modelling: a comprehensive framework for principal coordinate analysis of neighbour matrices (PCNM). *Ecological Modelling*, **196**(**3–4**): 483–493.

Durrant, H.M., Barrett, N.S., Edgar, G.J., Coleman, M.A. & Burridge, C.P. (2018). Seascape habitat patchiness and hydrodynamics explain genetic structuring of kelp populations. *Marine Ecology Progress Series*, **587**: 81–92.

Eger, A.M., Marzinelli, E.M., Beas-Luna, R., Blain, C.O., Blamey, L.K., Byrnes, J.E., Carnell, P.E., Choi, C.G., Hessing-Lewis, M., Kim, K.J., Kumagai, N.H., Lorda, J., Moore, P., Nakamura, Y., Pérez-Matus, A., Pontier, O., Smale, D., Steinberg, P.D. & Vergés, A. (2023). The value of ecosystem services in global marine kelp forests. *Nature Communications*, **14**(**1**): 1894.

Excoffier, L., Laval, G. & Schneider, S. (2005). Arlequin (version 3.0): an integrated software package for population genetics data analysis. *Evolutionary Bioinformatics Online*, **1**: 47–50.

Feldmann, J. (1937). *Recherches sur la végétation marine de la Méditerranée. La Côte des Albères*. PhD, University of Paris, France.

Fouqueau, L., Reynes, L., Tempera, F., Bajjouk, T., Blanfuné, A., Chevalier, C., Laurans, M., Mauger, S., Sourisseau, M., Assis, J., Lévêque, L. & Valero, M. (2024). Seascape genetic study on *Laminaria digitata* underscores the critical role of sampling schemes. *Marine Ecology Progress Series*, **740**: 23–42.

Fragkopoulou, E., Serrão, E.A., De Clerck, O., Costello, M. J., Araújo, M.B., Duarte, C.M., Krause-Jensen, D. & Assis, J. (2022). Global biodiversity patterns of marine forests of brown macroalgae. *Global Ecology and Biogeography*, **31**(**4**): 636–648.

Fraschetti, S., Terlizzi, A., Guarnieri, G., Pizzolante, F., D'Ambrosio, P., Maiorano, P., Beqiraj, S. & Boero, F. (2011). Effects of unplanned development on marine biodiversity: a lesson from Albania (central Mediterranean Sea). *Journal of Coastal Research*, **58**: 106–115.

Gianni, F., Bartolini, F., Pey, A., Laurent, M., Martins, G.M., Airoldi, L. & Mangialajo, L. (2017). Threats to large brown algal forests in temperate seas: the overlooked role of native herbivorous fish. *Scientific Reports*, **7**(**1**): 6012.

Gouvêa, L.P., Fragkopoulou, E., Cavanaugh, K., Serrão, E. A., Araújo, M.B., Costello, M.J., Westergerling, E.H.T. & Assis, J. (2023). Oceanographic connectivity explains the intra-specific diversity of mangrove forests at global scales. *Proceedings of the National Academy of Sciences*, **120**(**14**): e2209637120.

Guzinski, J., Ballenghien, M., Daguin-Thiébaut, C., Lévêque, L. & Viard, F. (2018). Population genomics of the introduced and cultivated Pacific kelp undaria pinnatifida: marinas—not farms—drive regional connectivity and establishment in natural rocky reefs. *Evolutionary Applications*, **11**(**9**): 1582–1597.

Guzinski, J., Ruggeri, P., Ballenghien, M., Mauger, S., Jacquemin, B., Jollivet, C., Coudret, J., Jaugeon, L., Destombe, C. & Valero, M. (2020). Seascape genomics of the sugar kelp *Saccharina latissima* along the North Eastern Atlantic Latitudinal Gradient. *Genes*, **11**(**12**): 1503.

Halkett, F., Simon, J.C. & Balloux, F. (2005). Tackling the population genetics of clonal and partially clonal organisms. *Trends In Ecology & Evolution*, **20**(**4**): 194–201.

Hanley, M.E., Firth, L.B. & Foggo, A. (2024). Victim of changes? Marine macroalgae in a changing world. *Annals of Botany*, **133**(**1**): 1–16.

Hoek, C., Mann, D.G. & Jahns, H.M. (1995). *Algae: An Introduction To Phycology*. Cambridge University Press, Cambridge.

Johnson, M.S. & Black, R. (1982). Chaotic genetic patchiness in an intertidal limpet, *Siphonaria* sp. *Marine Biology*, **70**: 157–164.

Kamvar, Z.N., Brooks, J.C. & Grünwald, N.J. (2015). Novel R tools for analysis of genome-wide population genetic data with emphasis on clonality. *Frontiers in Genetics*, **6**: 151034.

Kamvar, Z.N., Tabima, J.F. & Grünwald, N.J. (2014). Poppr: an R package for genetic analysis of populations with clonal, partially clonal, and/or sexual reproduction. *Peerj*, **2**: e281.

Keenan, K., McGinnity, P., Cross, T.F., Crozier, W.W. & Prodöhl, P.A. (2013). DiveRsity: an R package for the estimation and exploration of population genetics parameters and their associated errors. *Methods in Ecology and Evolution*, **4**(**8**): 782–788.

Kool, J.T., Paris, C.B., Andréfouët, S. & Cowen, R.K. (2010). Complex migration and the development of genetic structure in subdivided populations: an example from Caribbean coral reef ecosystems. *Ecography*, **33**(**3**): 597–606.

Krueger-Hadfield, S.A., Collen, J., Daguin-Thiébaut, C. & Valero, M. (2011). Genetic population structure and mating system in *Chondrus crispus* (Rhodophyta). *Journal of Phycology*, **47**: 440–450.

Ledoux, J.-B., Mokhtar-Jamaï, K., Roby, C., Féral, J.P., Garrabou, J. & Aurelle, D. (2010). Genetic survey of shallow populations of the Mediterranean red coral [*Corallium rubrum* (Linnaeus, 1758)]: new insights into evolutionary processes shaping nuclear diversity and implications for conservation. *Molecular Ecology*, **19**: 675–690.

Legendre, P. & Anderson, M.J. (1999). Distance-based redundancy analysis: testing multispecies responses in multifactorial ecological experiments. *Ecological Monographs*, **69**(**1**): 1–24.

Legrand, T., Chenuil, A., Ser-Giacomi, E., Arnaud-Haond, S., Bierne, N. & Rossi, V. (2022). Spatial coalescent connectivity through multi-generation dispersal modelling predicts gene flow across marine phyla. *Nature Communications*, **13**(**1**): 5861.

Legrand, T., Fragkopoulou, E., Vapillon, L., Gouvêa, L., Serrão, E.A. & Assis, J. (2024). Unravelling the role of oceanographic connectivity in the distribution of genetic diversity of marine forests at the global scale. *Global Ecology and Biogeography*, **33**: e13857.

Lenormand, T. (2002). Gene flow and the limits to natural selection. *Trends in Ecology & Evolution*, **17**(**4**): 183–189.

Li, G. & Hedgecock, D. (1998). Genetic heterogeneity, detected by PCR-SSCP, among samples of larval Pacific oysters (*Crassostrea gigas*) supports the hypothesis of large variance in reproductive success. *Canadian Journal of Fisheries and Aquatic Sciences*, **55**(**4**): 1025–1033.

Manca, F., Benedetti-Cecchi, L., Bradshaw, C.J., Cabeza, M., Gustafsson, C., Norkko, A.M. & Strona, G. (2024). Projected loss of brown macroalgae and seagrasses with global environmental change. *Nature Communications*, **15**(**1**): 5344.

Mangialajo, L., Chiantore, M., Susini, M.L., Meinesz, A., Cattaneo-Vietti, R. & Thibaut, T. (2012). Zonation patterns and interspecific relationships of fucoids in microtidal environments. *Journal of Experimental Marine Biology and Ecology*, **412**: 72–80.

Marchiori, M. & Latora, V. (2000). Harmony in the small-world. *Physica A: Statistical Mechanics and Its Applications*, **285**(**3–4**): 539–546.

Minne, A.J., Vranken, S., Wheeler, D., Wood, G., Batley, J., Wernberg, T. & Coleman, M.A. (2025). Strong environmental and genome-wide population differentiation underpins adaptation and high genomic vulnerability in the dominant Australian kelp (*Ecklonia radiata*). *Ecology and Evolution*, **15**(**5**): e71158.

Monserrat, M., Comeau, S., Verdura, J., Alliouane, S., Spennato, G., Priouzeau, F. & Mangialajo, L. (2022). Climate change and species facilitation affect the recruitment of macroalgal marine forests. *Scientific Reports*, **12** (**1**): 18103.

Neiva, J., Bermejo, R., Medrano, A., Capdevila, P., Milla-Figueras, D., Afonso, P., Ballesteros, E., Sabour, B., Serio, D., Nobrega, E., Soares, J., Valdazo, J., Tuya, F., Mulas, M., Israel, A., Sadogurska, S.S., Guiry, M.D., Pearson, G. A. & Serrão, E.A. (2022). DNA barcoding reveals cryptic diversity, taxonomic conflicts, and novel biogeographical insights in *Cystoseira* s.l (Phaeophyceae). *European Journal of Phycology*, **58**(**3**): 351–375.

Neiva, J., Pearson, G.A., Valero, M. & Serrao, E.A. (2012). Drifting fronds and drifting alleles: range dynamics, local dispersal, and habitat isolation shape the population structure of the estuarine seaweed *Fucus ceranoides*. *Journal of Biogeography*, **39**(**6**): 1167–1178.

Oksanen, J. (2010). Vegan: community ecology package. Retrieved September 2025 from http://vegan.r-forge.r-project.org/

Pineda, J., Hare, J.A. & Sponaugle, S. (2007). Larval transport and dispersal in the coastal ocean and consequences for population connectivity. *Oceanography*, **20**(**3**): 22–39.

Raymond, M. & Rousset, F. (1995). GENEPOP (version 1.2): population genetics software for exact tests and ecumenicism. *Journal of Heredity*, **86**: 248–249.

Reynes, L., Aurelle, D., Chevalier, C., Pinazo, C., Valero, M., Mauger, S., Sartoretto, S., Blanfuné, A., Ruitton, S., Boudouresque, C.F., Verlaque, M. & Thibaut, T. (2021a). Population genomics and Lagrangian modeling shed light on dispersal events in the Mediterranean endemic *Ericaria zosteroides* (= *Cystoseira zosteroides*) (Fucales). *Frontiers In Marine Science, Section Marine Molecular Biology and Ecology*, **8**: 683528.

Reynes, L., Fouqueau, L., Aurelle, D., Mauger, S., Destombe, C. & Valero, M. (2024). Temporal genomics help in deciphering neutral and adaptive patterns in the contemporary evolution of kelp populations. *Journal of Evolutionary Biology*, **37**(**6**): 677–692.

Reynes, L., Thibaut, T., Mauger, S., Blanfuné, A., Holon, F., Cruaud, C. & Aurelle, D. (2021b). Genomic signatures of clonality in the deep water kelp *Laminaria rodriguezii*. *Molecular Ecology*, **30**(**8**): 1806–1822.

Riquet, F., De Kuyper, C.A., Fauvelot, C., Airoldi, L., Planes, S., Fraschetti, S., Macic, V., Milchakova, N., Mangialajo, L. & Bottin, L. (2021). Highly restricted dispersal in habitat-forming seaweed may impede natural recovery of disturbed populations. *Scientific Reports*, **11**(**1**): 16792.

Robvieux, P., 2013. *Conservation des populations de* Cystoseira *en régions Provence-Alpes-Côte-d'Azur et Corse*. PhD Thesis, Université Nice Sophia Antipolis, France.

Robvieux, P., Videment, J., Ribout, C., Forcioli, D., Meinesz, A., Thibaut, T. & Bottin, L. (2012). First characterization of eight polymorphic microsatellites for *Cystoseira amentacea* var. *stricta* (Fucales, Sargassaceae). *Conservation Genetics Resources*, **4**: 923–925.

Ronce, O. & Kirkpatrick, M. (2001). When sources become sinks: migrational meltdown in heterogeneous habitats. *Evolution*, **55**(**8**): 1520–1531.

Rousset, F. (2008). Genepop'007: a complete re-implementation of the genepop software for Windows and Linux. *Molecular Ecology Resources*, **8**(**1**): 103–106.

Ryman, N. (1997). Minimizing adverse effects of fish culture: understanding the genetics of populations with overlapping generations. *ICES Journal of Marine Science*, **54**(**6**): 1149–1159.

Sala, E. & Knowlton, N. (2006). Global marine biodiversity trends. *Annual Review of Environment and Resources*, **31**: 93–122.

Slatkin, M. (1985). Gene flow in natural populations. *Annual Review of Ecology and Systematics*, **16**(**1**): 393–430.

Slatkin, M. (1987). Gene flow and the geographic structure of natural populations. *Science*, **236**(**4803**): 787–792.

Steneck, R.S., Graham, M.H., Bourque, B.J., Corbett, D., Erlandson, J.M., Estes, J.A. & Tegner, M.J. (2002). Kelp forest ecosystems: biodiversity, stability, resilience, and future. *Environmental Conservation*, **29**(**4**): 436–459.

Susini, M.L. (2006) *Statut et biologie de* Cystoseira amentacea *var.* stricta. PhD, University of Nice-Sophia Antipolis, France.

Susini, M.L., Thibaut, T., Meinesz, A. & Forcioli, D. (2007). A preliminary study of genetic diversity in *Cystoseira amentacea* (C.Agardh) Bory var. *stricta* Montagne (Fucales, Phaeophyceae) using random amplified polymorphic DNA. *Journal Information*, **46**: 406–411.

Thibaut, T., Blanfuné, A., Markovic, L., Boudouresque, C.F. & Verlaque, M. (2015). Decline and local extinction of Fucales in French Riviera: the harbinger of future extinctions? *Mediterranean Marine Science*, **16**(**1**): 206–224.

Thibaut, T., Blanfuné, A., Markovic, L., Verlaque, M., Boudouresque, C.F., Perret-Boudouresque, M., Macic, V. & Bottin, L. (2014). Unexpected abundance and long-term relative stability of the brown alga *Cystoseira amentacea*, hitherto regarded as a threatened species, in the north-western Mediterranean Sea. *Marine Pollution Bulletin*, **89**(**1–2**): 305–323.

Thibaut, T., Bottin, L., Aurelle, D., Boudouresque, C.F., Blanfuné, A., Verlaque, M., Pairaud, I. & Millet, B. (2016). Connectivity of populations of the seaweed *Cystoseira amentacea* within the Bay of Marseille (Mediterranean Sea): genetic structure and hydrodynamic connections. *Cryptogamie Algologie*, **37**(**4**): 233–255.

Toonen, R.J. & Hughes, S. (2001). Increased throughput for fragment analysis on an ABI PRISM® 377 automated sequencer using a membrane comb and strand software. *Biotechniques*, **31**: 1320–1325.

Van Oosterhout, C., Hutchinson, W.F., Wills, D.P. & Shipley, P. (2004). MICRO-CHECKER: software for identifying and correcting genotyping errors in microsatellite data. *Molecular Ecology Notes*, **4**(**3**): 535–538.

Vranken, S., Wernberg, T., Scheben, A., Severn-Ellis, A.A., Batley, J., Bayer, P.E., Edwards, D., Wheeler, D. & Coleman, M.A. (2021). Genotype–Environment mismatch of kelp forests under climate change. *Molecular Ecology*, **30**(**15**): 3730–3746.

Whitlock, M.C. (2011). G'ST and D do not replace FST. *Molecular Ecology*, **20**(**6**): 1083–1091.

Winter, D.J. (2012). MMOD: an R library for the calculation of population differentiation statistics. *Molecular Ecology Resources*, **12**(**6**): 1158–1160.